Intercalation by atoms of a two-dimensional graphite film on a metal

A. Ya. Tontegode and E. V. Rut'kov

A. F. Ioffe Physicotechnical Institute, Russian Academy of Sciences, St. Petersburg
(Submitted 15 July 1993; resubmitted after revision 20 September 1993)
Usp. Fiz. Nauk. **163**, 57–74 (November 1993)

Intercalation by atoms (Cs, K, Ba, Pt, Si, C,...) of a monolayer graphite film deposited on a metal (Ir, Re,...) is reviewed. Atoms with low ionization potential (Cs, K, Ba,...) form a monolayer film of the intercalate under the graphite layer, whereas atoms with high unionization potential (Pt, Si, C,...) form a thick multilayer film. The high intercalation efficiency can be accounted for by weak bonding (physisorption) of the graphite film to the metal. An intercalation mechanism is proposed. The superefficient diffusion of intercalated atoms into metals is discussed.

INTRODUCTION

Contact between a hot metal and a carbon-containing medium is often accompanied by the release of surface carbon which can take a variety of forms, including C-atoms, C-clusters, surface carbide, and graphite.[1] Of these, only graphite is valence saturated, so that the formation of a two-dimensional graphite film on the surface of a metal gives rise to a number of striking effects. Thus, a graphite monolayer will completely poison platinum metal catalysts in molecular dissociation reactions.[1,2] Only weak physisorption of multivalent atoms of transition metals (Mo, Pt, Ni) is observed on a graphite monolayer on a metal.

Metals with a two-dimensional graphite surface film are frequently encountered throughout science and technology, e.g., in heterogeneous catalysis, vacuum and electrovacuum technology, and the properties of metals. A two-dimensional graphite film is formed on the low-index surfaces of metals with different crystal geometry, i.e., fcc (Ir, Pt, Ni, Rh,...), bcc (Mo,...), and hcp (Re, Ru,...), under exposure to hydrocarbon vapor at elevated temperatures.[1] For example, benzene molecules (C_6H_6) dissociate on the (111) surface of iridium at 1300 K, hydrogen is desorbed, and C-atoms form graphite islands and a graphite monolayer. The thickness of the graphite film ceases to grow beyond the monolayer value because valence saturation of the film ensures that the C_6H_6 molecules do not dissociate on the film. Because of their common occurrence and importance, it is interesting to examine the physicochemical properties of film systems of the form metal plus two-dimensional graphite film, and to examine transport processes in such systems.

This review is devoted to a new phenomenon discovered in recent years, namely, intercalation by atoms of a two-dimensional graphite film on a metal surface. The adsorption of potassium atoms on a monolayer graphite film of iridium (Ir–C) was unexpectedly found to exhibit the phenomenon of intercalation, i.e., the spontaneous penetration of the film by atoms adsorbed on the two-dimensional graphite film until they are found under the film.[3,4] This is the first published review of research into the intercalation by atoms of a two-dimensional graphite film of the metal. The review summarizes the results obtained by the group led by A. Ya. Tontegode at the A. F. Ioffe Physicotechnical Institute of the Russian Academy of Sciences, who discovered intercalation of (Ir–C) by potassium and investigated it in detail. They also examined intercalation of (Ir–C) and (Re–C) by many other atoms (K, Cs, Ba, Sr, Pt, Si, C, Ag, Cu, Ir, Mo). Their research has revealed the basic properties of the phenomenon and suggested a mechanism for it. It has also indicated possible practical applications.

In addition to presenting a discussion of experimental results, we shall examine two fundamental problems that govern the physics of intercalation. The first concerns the nature of adsorption bonding between graphite islands and the metal surface, which has been shown[1] to take the form of physisorption under the influence of van der Waals forces (without electron exchange). The second is the special mechanism of intercalation by atoms of a two-dimensional graphite film on a metal, which can probably be extended to the intercalation of crystalline graphite (HOPG) and other layered materials (MoS_2 etc.).

EXPERIMENTAL RESULTS

2.1. The character of intercalation of crystalline graphite

We start by summarizing basic information about intercalation of graphite in bulk. The spontaneous penetration of certain atoms and molecules from outside crystalline graphite into its internal interlayer region, i.e., intercalation, is a widely known phenomenon that is exploited in the synthesis of new highly anisotropic solid with a variety of electromagnetic, optical, and other properties that are of considerable importance in many scientific and practical applications.[5–10] Highly oriented pyrolitic graphite (HOPG) is often used in intercalation. The average size of crystallites in the basal plane is about 1 μm and the sample volume can amount to a few cubic centimeters. For example, exposure of hot HOPG to cesium vapor results in

 1063-7869/93/111053-15$10.00

the spontaneous penetration of cesium into the layered structure and, in the final stage, the formation of the intercalated compound C_8Cs in which graphite layers with concentration $N_C=3.86\times10^{15}$ cm^{-2} alternate with cesium layers with $N_{Cs}=5\times10^{-14}$ cm^{-2}, the separation between neighboring graphite layers being raised from 3.35 Å in the crystalline graphite to 5.94 Å in C_8Cs. An important specific property of intercalated compounds of graphite is the preservation of the structure and lattice constant of a graphite layer, i.e., of its individuality.

Only certain atoms and particular classes of molecules undergo direct intercalation of graphite. Several hundred such particles are known. Depending on the direction of the transition of the valence electron between the intercalated particle and the graphite valence band, we have donor intercalates (Cs, Rb, K, Li, Ba, Eu,...) and acceptor intercalates (Br_2, F_2, the metal chlorides $FeCl_3$, $AlCl_3$, $CoCl_2$, $NiCl_2$ and the metal fluorides TiF_4, NbF_5, WF_6, and also HNO_3, H_2SO_4, N_2O_5, AsF_5, etc.). Biintercalates have been found and investigated. For example, the Bi, As, Sb, Tl, and Hg atoms do not directly intercalate HOPG, but they penetrate the hot graphite lattice in the form of a mixture of the vapor of these atoms and an alkali metal, e.g., potassium, forming a binary alloy in the intercalated state in which two-dimensional layers alternate in the following sequence: graphite, K, Hg, K, graphite. Biintercalates containing both metal and hydrocarbon molecules have also been found, for example, *n*-hexane in the second phase of $C_{24}Cs$.

An important topic in research into the industrial application of intercalated compounds of graphite is the development of low-resistance media for electrical engineering. Two types of graphite material are used for this purpose, namely, graphite fibers and HOPG. Their resistivity is reduced as a result of intercalation by acceptor impurities (F_2, B_2, metal chlorides, and AsF_5) which reduce the resistivity practically to that of copper. They are used as electrode materials in electrolysis, in batteries, and so on.

Regular international symposia devoted to the problem of intercalated graphite compound are being held. Most studies are concerned with intercalated HOPG whereas the intercalation of a two-dimensional graphite film on a metal surface was discovered and investigated by our group. This is a particular form of intercalation that has common features with, and significant differences from, the intercalation of HOPG.[11,12] For example, atoms with high ionization potential Pt, Si, C,... intercalate the two-dimensional graphite form and form a thick intercalate film under it. The latter is not produced during the intercalation of HOPG. Atoms with low ionization potentials (Cs, K, Ba,...) similarly intercalate HOPG and the two-dimensional graphite film. We suggest that the thermal bubble mechanism developed in Ref. 13 for the two-dimensional graphite film can be extended to the intercalation of HOPG for which the mechanism has not as yet been established.

We now turn to the presentation of experimental results on the intercalation by atoms of a two dimensional graphite film on a metal.

2.2. Intercalation of Ir–C by potassium[3,4,14]

The adsorption of potassium atoms by a monolayer of graphite on iridium[3-4] in the form of thin tapes, textured with the (111) surface and having a work function $\varphi=5.75$ eV, has been investigated in ultrahigh vacuum. The graphite monolayer was produced by exposing iridium at 1600 K to benzene. We note that surface carbon does not dissolve in iridium, but desorbs at temperatures $T\geqslant2000$ K (Ref. 1). The surface was analyzed by high-resolution Auger electron spectroscopy (AES) with ($\Delta E/E\geqslant0.1\%$) and ion-burst thermal desorption spectroscopy (TDS), using K^+ detection. The K^+ ions can be detected with high efficiency ($\leqslant100\%$) by means of surface ionization[15] which transforms the potassium atoms during desorption, thus increasing the detection sensitivity by a factor of about 1000 (the work function of a monolayer of graphite on iridium is $5=4.45$ eV). Another phenomenon that was used was the "neutral burst" in which atoms are ionized by electron impact.

When potassium atoms are deposited on a graphite monolayer on hot iridium, and then the ion burst is produced at 2200 K, the thermal desorption spectrum exhibits three phases (α, β, and γ). It is found that the α-phase is formed by potassium adsorbed on the graphite monolayer and desorbed at temperatures $T\leqslant900$ K. The β-phase, which has low adsorption capacity, is formed by potassium atoms decorating the edge of the graphite islands which are desorbed at $T\leqslant500$ K (in accordance with Ref. 16). The very unusual γ-phase, from which potassium is desorbed at the record high temperatures $T<2000$ K is formed by potassium located under the graphite monolayer in the intercalated state. It is shown in Ref. 14, that γ-phase potassium is indeed located under the graphite monolayer (for example, potassium from the γ-phase reduces the Auger peak of iridium, but not the Auger peak of carbon).

The α-, β-, and γ-phases are filled in a particular sequence. The α- and β-phases are filled first. After the potassium concentration $N_\alpha\sim5\times10^{11}$ cm^{-2} has been reached on the surface of the graphite layer, the filling of the γ-phase begins simultaneously with the filling of the α- and β-phases. Figure 1 illustrates the successive filling with potassium of the difference phases of a graphite monolayer of iridium at 300 K in a potassium beam with $\nu_K=1.6\times10^{12}$, cm^{-2} s^{-1}. It is clear that N_γ is comparable with $N_\alpha+N_\beta\approx N_\alpha$; at the end of adsorption, $N_\alpha\approx N_\beta\approx3\times10^{14}$ cm^{-2}. It is found that the calculated concentration $N=\nu_K t$ of potassium atoms that enter the α-phase of the iridium tape is greater by a factor of two than the true concentration $N_\alpha+N_\beta+N_\gamma$ of adatoms of potassium upon it. Consequently, at 300 K, the potassium adatoms already effectively migrate over the graphite monolayer and are divided equally between the two sides of the tape, filling the α- and γ-phases on its rear with $N_\alpha\approx N_\gamma$. We now define the intercalation efficiency $\varkappa$ as the fraction of particles incident on the graphite monolayer

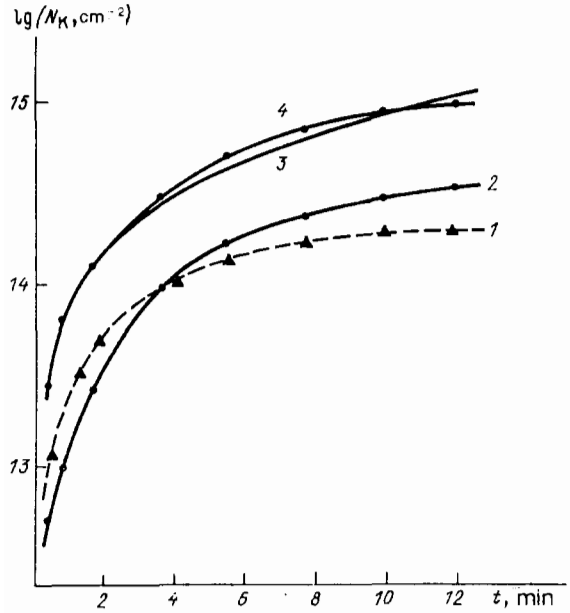

FIG. 1. Adsorption of potassium atoms ($\nu_K = 1.6\times10^{12}$ cm^{-2} s^{-1}) on a graphite monolayer on iridium at $T=300$ K. Concentration of potassium atoms: *1*—N_γ ("neutral" burst), *2*—$N_\gamma+N_\beta$ (ion burst), *3*—calculated concentration $N=\nu_K t$, *4*—$2(N_\alpha+N_\beta+N_\gamma)$.

that penetrate it to the other side ($\varkappa = N_{int}/N_{inc}$). The intercalation efficiency is high (0.5) during the adsorption of potassium on Ir–C at 300 K.

The filling of the γ-phase on Ir–C at different iridium temperatures in a potassium beam of constant flux density ν_K at time t is shown in Fig. 2. For temperatures in the range $300 < T < 500$ K we observe the maximum possible filling of the γ-phase with $N_\gamma \sim 3\times10^{14}$ cm^{-2} which is independent of ν_K and t, and the intercalation efficiency is 0.5. At higher temperatures, $900 < T < 1600$ K, the intercalation efficiency is close to $R \sim 5\times10^{-4}$ and is practically

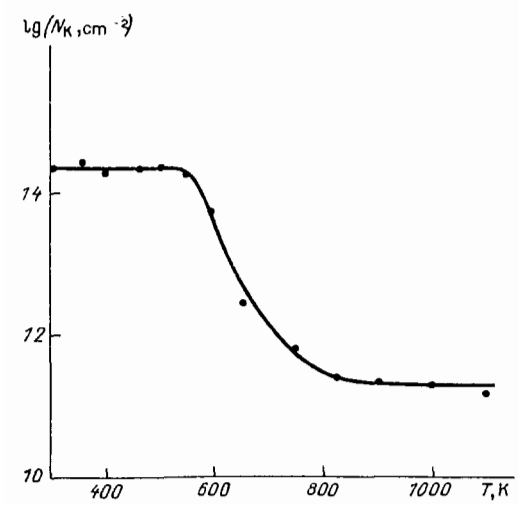

FIG. 2. Concentration of potassium atoms in the γ-phase for a graphite monolayer on iridium, kept in a potassium flux $\nu_K = 6\times10^{11}$ cm^{-2} s^{-1} for $t=10$ min as a function of temperature T.

independent of temperature whilst N_γ is directly proportional to ν_K and to the exposure time. It is probable that $\varkappa \sim 5\times10^{-4}$ is the fraction of the surface occupied by the edges of the graphite islands from which atoms deposited on the surface undergo a transition to the intercalated state. Since we know that at the end of the adsorption of potassium on Ir–C at 3300 K, the densities of the α- and β-phases are $N_\alpha = 3\times10^{14}$ and $N_\beta = 3\times10^{11}$ cm^{-2}, we can independently calculate the fraction of the surface area occupied by the edges of the graphite islands. The result is $N_\beta/N_\alpha \cong 6\times10^{-4}$, which is close to the above figure of $\varkappa \sim 5\times10^{-4}$. If we suppose that the potassium adatom has a diameter of $a=3$ Å, we can use N_α and N_β to estimate the radius R of a graphite island and the concentration f of such islands. Since $N_\beta = 2\pi R\cdot f/a$ and $\pi R^2\cdot f = a^2 N_\alpha$ we have $R = 2aN_\alpha/N_\beta = 9000$ Å and $f = 10^{16}$ Å$^2/\pi R^2 = 4\times10^7$ cm^{-2}.

The sharp rise in N_α for $T < 700$ K with $\nu_K = \text{const}$ is due to the increase in the surface concentration of the potassium adatoms to a level ($\theta > 0.01$) at which the electrostatic repulsion between the K^+ adatoms ensures that they diffuse efficiently under the graphite islands.

At $T = 1500$ K, a potassium-ion flux of density ν continuously desorbs from the iridium surface covered with the graphite monolayer and filled with the γ-phase. This may be intercalated potassium migrating from under the edges of the graphite islands (when $N_\gamma \sim 2.5\times10^{13}$ cm^{-2}, we have $\gamma \sim 2\times10^8$ cm^{-2} s^{-1}).

Intercalation due to adsorption of potassium on iridium was investigated in Ref. 4 and 14 and the graphite islands were found to occupy a fraction $0 < s'' < 1$ of the area. This fraction was determined from the dissociation of CsCl molecules.[1,2,15] The transition from the continuous graphite layer to the graphite islands is accompanied by the appearance of a number of features in the thermal desorption spectra (Fig. 3a). First, there is a sharp increase in the amount of the β-phase (from $N_\beta \sim 2\times10^{11}$ cm^{-2} on the graphite monolayer to $N_\beta \approx 4\times10^{13}$ cm^{-2} at the maximum of the function $\log N_\beta(f)s''$, when the surface at 800 K adsorbed potassium flux rate $\nu_K = 10^{12}$ cm^{-2} s^{-1} for 10 min. Second, as the fraction $1-s''$ of the area free from graphite islands increases, there is an accompanying rapid increase in the potassium adsorption time necessary to reach the onset of filling of the γ-phase. If we suppose that all the potassium atoms reaching the surface of the graphite islands "roll" on to the iridium, then we find that, for all s'', the filling of the γ-phase begins for the same potassium concentration on iridium, namely, about 2.5×10^{12} cm^{-2} (on Ir–C, intercalation begins at the concentration of 5×10^{11} cm^{-2}).

Let us now explain these results. Iridium covered by graphite islands contains a variety of adsorbed centers. For example, measurements of the lifetime of potassium adatoms in this system were used in Ref. 16 to detect adsorption centers with enhanced bonding energies to potassium adatoms in the range $2.4 < E < 3.0$ eV. The energy of 3.0 eV was identified with potassium atoms decorating the edges of the graphite islands. The lower energies in this range were associated with potassium atoms adsorbed on chem-

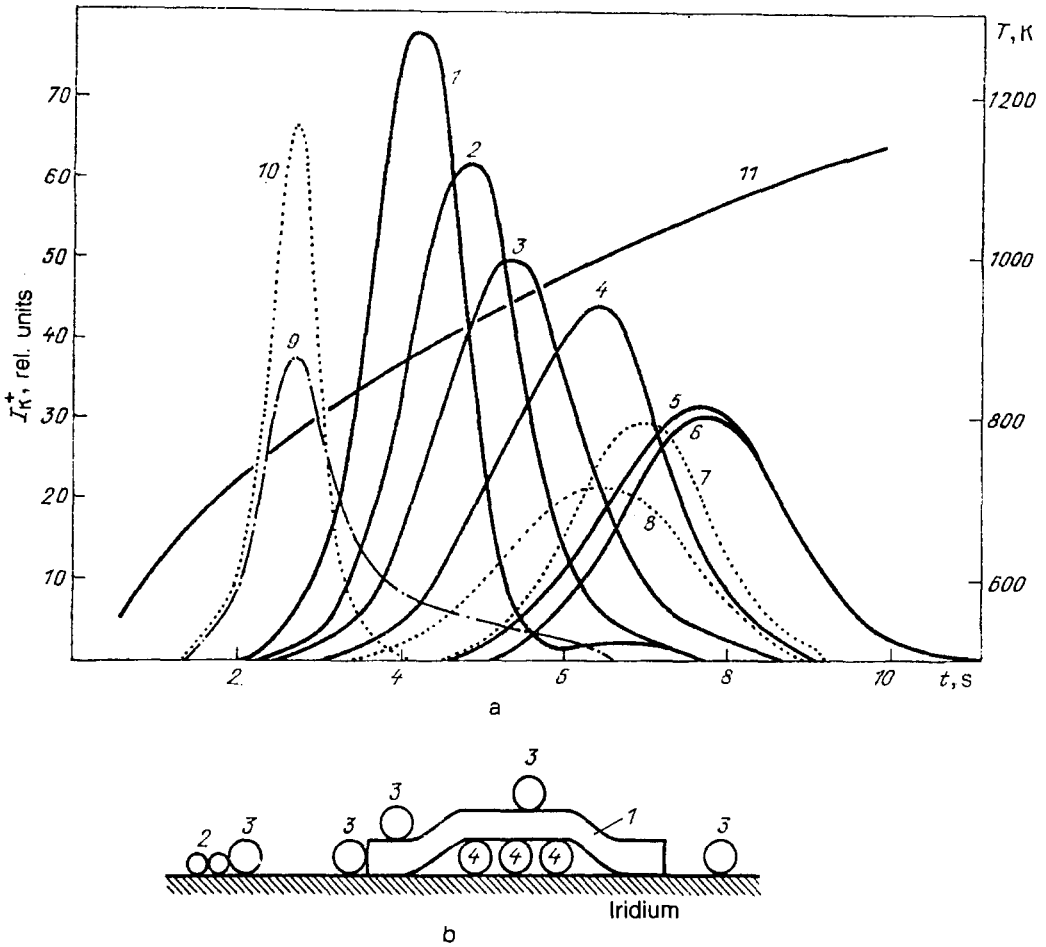

FIG. 3. a—Thermal desorption spectra of K^+ ions for iridium with graphite islands, held at 300 K in potassium vapor with $\nu_K = 2.8\ cm^{-2}\ s^{-1}$ for $t = 30$ s. Relative area of graphite islands: *1*—<0.01; *2*—0.03; *3*—0.07; *4*—0.14; *5*—0.50; *6*—0.71; *7*—0.89; *8*—0.93; *9*—<1; *10*—1; *11*—the function $T(t)$. b—Model of iridium surface with a graphite island (*1*), carbon cluster (*2*), and adsorbed (*3*) and intercalated (*4*) potassium atoms.

ically active carbon clusters (doublets, triplets, etc., i.e., small aggregates of C-atoms, chemisorbed from iridium; Fig. 3b). Adsorption centers with the highest bonding energy (edges of islands and carbon clusters) should be the first to be filled during the adsorption of potassium in the presence of migration. These adatoms form the β-phase during thermal desorption. The wide β-phase peak suggests that the adsorption bonding energy lies in a wide interval. Once the β-phase has been filled, the subsequent potassium atoms fill less energetically favorable centers, i.e., they are adsorbed on iridium (α_2-phase). During thermal disorption, α_2- is the first to be desorbed, followed by the β-phase. For still greater exposures, the α_1-phase begins to fill, i.e., the potassium atoms are adsorbed on the surface of the graphite islands. Coulomb repulsion between positively charged potassium adatoms that prevent the filling of the adlayer undoubtedly plays a significant role for $\beta > 0.1$. This probably ensures that the potassium monolayer on iridium is not fully filled and potassium atoms arriving on the surface for $N \sim 2.5 \times 10^{14}\ cm^{-2}$ begin to occupy the free surface of the graphite islands which are intercalated by them by analogy with the intercalation by potassium of the graphite monolayer of iridium.

2.3. Intercalation by cesium by Rb–C (Refs. 17–21) and Ir–C (Refs. 22–25)

Following the publication of the discovery and investigation of the intercalation by potassium of the graphite monolayer on iridium[3,4,14] attempts were made to establish whether intercalation by cesium of a graphite monolayer on rhenium was possible for different intercalated particles and substrate metals. The technique used in Refs. 3, 4, and 14, was employed once again. Thin textured rhenium tapes with the (10–10) face on the surface and work function $e\varphi = 5.15$ eV were investigated. The graphite monolayer was produced by the adsorption of benzene on hot (1700 K) rhenium saturated with carbon.[26] The rhenium was then rapidly cooled down to 300 K at which bulk diffusion of carbon was frozen and the graphite monolayer remained on the surface (C diffusion was unfrozen only for $T > 1200$ K). Cesium was adsorbed on Re–C with $e\varphi = 4.45$ eV and the system was investigated by AES and DTS. It was found that Cs efficiently intercalates Re–C and that this is in many ways similar to the intercalation by potassium of Ir–C. Thus, during the adsorption of cesium on Re–C in the temperature range $300 < T < 600$ K, the intercalation

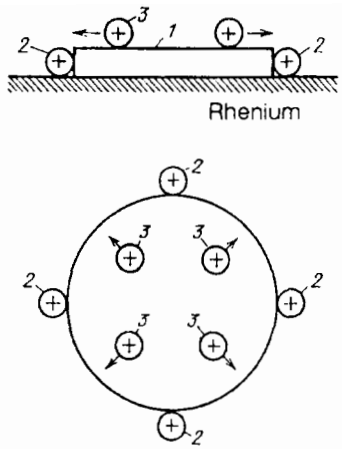

FIG. 4. Model of the rhenium surface with graphite island (*1*), Cs^+ adions decorating the island (*2*), and Cs^+ adions adsorbed on the island (*3*).

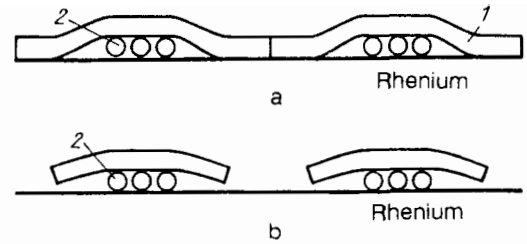

FIG. 5. Model of a graphite monolayer (*1*) on rhenium with intercalated cesium (*2*) at carbonization temperature T_d (a) after heating to $T > T_d$ (b).

efficiency is high (0.5) and a monotonic intercalate is formed under the graphite monolayer with a concentration of about 4×10^{14} cm^{-2}. When cesium is absorbed on Re–C at temperatures in the range $900 < T < 1200$ K, the intercalation efficiency falls to $\varkappa \sim 10^{-4}$ and is independent of T.

The huge difference between the thermal stability of adsorbed and intercalated cesium found by investigating Re–C is exceedingly interesting. Adsorbed cesium is desorbed at low temperatures of ($T \sim 1800$ K) whereas intercalated cesium escape only at the record high temperatures of $T \sim 2200$ K. This persistent presence of cesium in contact with the hot metal will find applications in practice and awaits a model interpretation.

The "ion burst" was used in Ref. 18 to investigate the migration of cesium on Re–C. It was found that for $N < 10^{12}$ cm^{-2} all the cesium adsorbed on Re–C at 300 K remains on the front face of the tape. For $N > 10^{12}$ cm^{-2}, the migration of cesium ensures that it is equally divided between the front and the rear surfaces of the tape. The absence of migration at 300 K for $N \ll 10^{12}$ cm^{-2} and the presence of cesium at higher concentrations shows that migration is due to Coulomb repulsion between the Cs^+ adions and is not due to thermal excitation. There is a concentration threshold, $N \geqslant 10^{13}$ cm^{-2} above which the cesium adatoms effectively fill the intercalated state (γ-phase) on the front and rear faces of the tape. The fact that there is a concentration threshold indicates a positive charging of the edge of the graphite island which, in contrast to the central portion of the island, is chemically active and is properly decorated by the Cs^+ ions (Fig. 4). As the concentration of cesium adsorbed on the graphite monolayer increases, there is an increase in the Coulomb repulsion between the Cs^+ adions. At the critical concentration, this enables the Cs^+ adatoms to approach the charged edge of the graphite island, which is necessary for intercalation.

Let us now examine the question of the effect of the intercalated cesium on the thermal stability of graphite islands on rhenium, which was discussed in Ref. 19. When the graphite monolayers produced on rhenium in benzene vapor at $T_c = 1700$ K is heated to 1800 K, it rapidly dissolves (in a matter of seconds). The question arises whether the intercalated cesium affects the rate at which the graphite monolayer is dissolved; for example, one might have expected, that when the temperature is raised to the above level, the monolayer will completely dissolve and the entire intercalated cesium will be desorbed as Cs^+ ions. It is found, however, that the Re–C–Cs system behaves in a different way. At 1800 K, a fraction of the graphite monolayer dissolves, but the remainder, containing the entire intercalated cesium, remains on the surface up to 2200 K, i.e., up to temperatures that are higher by about 500° than the carbonization temperature (when $N_\gamma = 8\times10^{13}$ cm^{-2}, the graphite island occupy about 40% of this surface). *Consequently, intercalated cesium prevents the graphite islands from desorbing and ensures that the islands display unique thermal stability.*

These results can be explained in terms of the model shown in Fig. 5. Figure 5a illustrates a graphite monolayer produced at $T_d = 1700$ K. It consists of a series of graphite islands containing the intercalated cesium and is physisorbed on rhenium. When the temperature is raised above T_d, the graphite layers begin to dissolve at the edges and the carbon adatoms diffuse into the rhenium metal. This dissolution process abruptly slows down when the island edges lift off as shown in Fig. 5b. Our experiments have shown that the bonding energy of an edge atom in a free graphite island, which is about 6.0 eV, is reduced to 3.0 eV on catalytically active rhenium surface. The C-atoms on the lifted edges break off at about 2200 K and this disrupts the island and frees the intercalated cesium.

The similarity between the intercalation of the graphite monolayer by cesium on iridium and on rhenium suggests that the nature of the metal on which the graphite monolayer is produced does not play an essential role in the intercalation phenomenon.

It was shown in Ref. 24 that exposure to radiation, or to electron bombardment, of a two-dimensional graphite film with intercalated cesium on iridium at about 900 K stimulates the escape of the adatoms from under the graphite islands. This escape was studied by Cs^+ ion current. The effect was observed at photon energies between 2.3 and 1.5 eV (the threshold on the low-energy side was not mea-

sured). It was assumed that adatoms escaped from under the graphite islands through "vents" produced when the bonding of edge C-atoms to iridium was disrupted by incident photons or electrons. The transport of particles in the absence of external stimulation was explained by diffusion through defects in the graphite layer. The kinetics of these light or electron stimulated processes was investigated in Ref. 25 and was explained in terms of a model. It was shown that a burst of Cs^+ ions was produced by the escape of adatoms from under the graphite monolayer near the edge of an island. The replenishment of the region near the edge of an island that has been depleted by radiation is a very slow process and probably takes place after the formation of a compact Cs atomic cluster that diffuses as whole towards the boundary of the island from its interior. An unusual migration of intercalated Cs atoms was thus established in Ref. 25: these atoms move in the form of compact clusters and not singly, and the rate of migration increases with increasing concentration of penetrated atoms.

2.4 Intercalation by barium of Ir–C (Refs. 27–30) and Re–C (Ref. 27) for $1000<T<1500$ K

It has been found that Ba intercalates a graphite monolayer on iridium or rhenium, but the character of the processes that take place is very dependent on the metal substrate temperature. We shall therefore consider these processes separately for $T<100$ K and $T>100$ K.

2.4.1. Adsorption of barium on Ir–C at $T<100$ K. It is probable that intercalation is observed during the adsorption of barium on iridium at 300 K. This follows from the characteristic change in the shape of the C_{kvv} Auger carbon peak (which will be discussed in detail in Sec. 2.10), but because of the strong Ba–Ba bonding on the surface of the graphite monolayer, we have barium condensation which interferes with the observation of the intercalation process. These difficulties are overcome when barium is adsorbed on heated Ir–C. For example, Fig. 6a shows the intensity of the Ba, Ir, and C Auger peaks during the adsorption of barium on Ir–C at 880 K (Ref. 27). The barium Auger peak grows during deposition, but the iridium peak declines whilst the carbon peak remains unaltered. This means that barium always accumulates under the graphite monolayer in the intercalated state (Fig. 6b). When $T>150$ s, the concentration of intercalated barium reaches 5×10^{13} cm^{-2} (which is close to its monolayer concentration on the surface of a transition metal) and ceases to vary. The intercalation efficiency is then about 0.3, i.e., 30% of the barium flux incident on the Ir–C surface becomes intercalated, whereas the remaining 70% is desorbed. When the system is heated, approximately 50% of the intercalated barium is desorbed for $T<1300$ K and the barium remaining under the graphite monolayer with a concentration of 2×10^{14} cm^{-2} escapes only for $T>2000$ K when the edges of the graphite islands are disrupted.

2.4.2. Adsorption of barium on Ir–C at $1000<T<1500$ K. Barium atoms with desorption activation energy of $E=1.9$ eV desorb efficiently from the graphite monolayer on iridium at 880 K. It was therefore surprising to find[31]

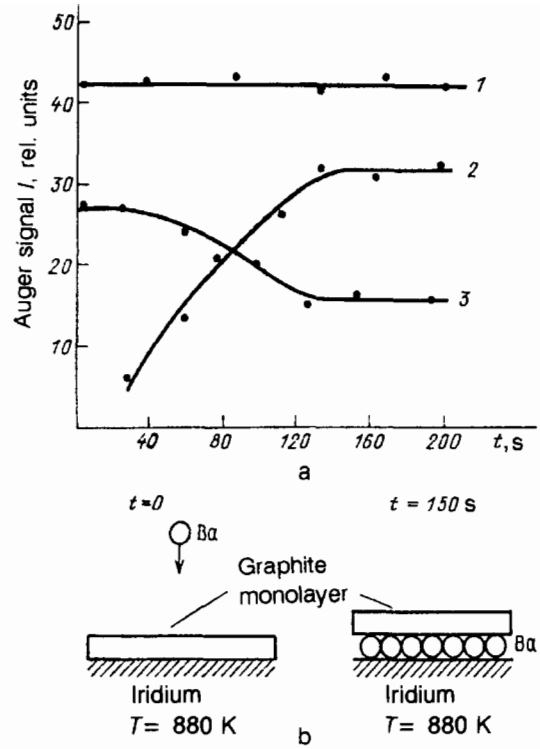

FIG. 6. a—Auger peak intensity for carbon (*1*), barium (*2*), and iridium (*3*) as a function of barium adsorption time for $\nu_{Ba}=10^{13}$–2×10^{13} cm^{-2} s^{-1} on a graphite monolayer on iridium at $T=880$ K. For $t>150$ s, the concentration of intercalated barium was $N_{Ba}\sim5\times10^{14}$ cm^{-2} s^{-1}. b—Model of the surface with adsorbed barium for $t=0$ and 150 s.

barium islands on Ir–C at the much higher temperatures in the range $100<T<1500$ K. A study was made of the growth and dissolution of two-dimensional barium islands on Ir–C (Refs. 31–34). The barium in these islands was strongly bonded to the substrate (with an energy of 3.4 eV) and had a high concentration (2×10^{11} cm^{-2}) although the barium islands were not closely packed. At these temperatures, the barium did not intercalate the graphite monolayer. The problem was to explain the high barium bonding energy to the substrate under islands (3.4 eV), which is much higher than the barium sublimation energy (about 1.80 eV) and the barium desorption energy on Ir–C (1.9 eV). We assume that the barium adatoms are adsorbed by benzene-ring centers in the graphite layer and as they undergo thermal oscillations, the adatoms approach the surface atoms of iridium, removing some of the graphite layer and becoming electron-bonded to iridium with bonding energy increased from 1.9 to 3.4 eV (Fig. 7).

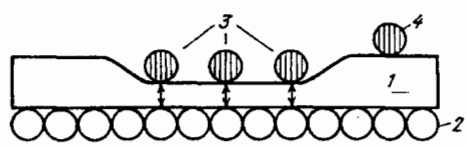

FIG. 7. Model of graphite monolayer (*1*) physisorbed on iridium (*2*) with strongly (*3*) and weakly (*4*) bonded barium atoms on the surface.

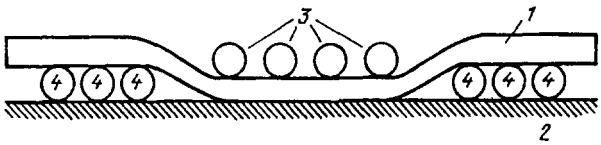

FIG. 8. Model of graphite monolayer (*1*) on iridium (*2*) with a two-dimensional island of barium (*3*) and intercalated barium (*4*).

This is a reasonable assumption since the desorption energy of a barium atom on the surface of iridium is high (5.7 eV). When this barium monolayer is heated to about 1600 K, about half of the available barium is desorbed and the rest is transferred under the monolayer to the intercalated state. Strongly-bonded barium islands are formed (but only on part of the surface,[27]) when the graphite monolayer containing intercalated barium with concentrations of 5×10^{11} cm^{-2} and temperatures in the range $100<T<1500$ K is again allowed to adsorb barium. The intercalated barium is probably nonuniformly distributed under the graphite monolayer in these experiments, and regions with maximum concentration of 5×10^{14} cm^{-2} are adjacent to regions in which there is no intercalated barium, and it is precisely in such regions that the strongly-bonded barium islands are formed on the graphite monolayer (Fig. 8). When the concentration of intercalated barium is $>2\times10^{14}$ cm^{-2}, strongly-bonded barium islands are not formed at all. it is also found that they are not formed on the surface of the graphite film on iridium when the film thickness is in excess of two monolayers. We have obtained similar results[35] for the adsorption of strontium on Ir–C.

2.5. Intercalation by Pt of Ir–C[36]

It turns out that the graphite monolayer with $e\varphi=4.45$ eV on metals (such as Ir and Re) is efficiently intercalated by atoms with low ionization potentials (Cs, K, Ba,...). Such atoms are positively charged on the graphite monolayer and are strongly bonded by image forces. We then have the interesting and important question: can a graphite monolayer on a metal be intercalated by atoms with high ionization potentials, which are not charged on the graphite monolayer and are weakly bonded by polarization-type van der Waals forces? To answer this question, we have investigated adsorption and intercalation of Ir–C by Pt, Si, and C atoms.

Platinum was deposited by sublimation from heated platinum strips. A thick platinum film was found to grow on a graphite monolayer during the adsorption of platinum on Ir–C at 300 K. It was found that the adsorption of platinum atoms on the graphite monolayer in iridium at 1000 K was accompanied by intercalation of Ir–C with efficiency $\varkappa=1$. This remarkable result means that, at 1000 K, *each platinum atom* incident on the graphite monolayer penetrates the layer and assumes the intercalated state under the layer. Figure 9a shows the variation in the height of the carbon-platinum and iridium Auger peaks during the adsorption of platinum on Ir–C at the higher temperature of 1200 K when the intercalation efficiency is somewhat

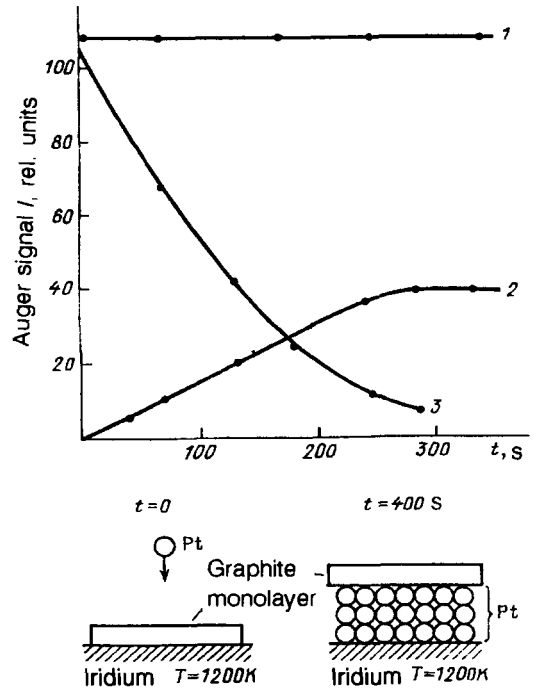

FIG. 9. A—Auger peak intensity for carbon (*1*), platinum (*2*), and iridium (*3*) as a function of time of deposition of platinum on a graphite monolayer on iridium at $T=1200$ K. b—Disposition of platinum atoms.

lower, $\varkappa<1$, and some of the platinum atoms desorb from the graphite monolayer. It is exceedingly interesting to note that, in contrast to Cs, K, and Ba atoms, which form a monolayer film in the intercalated state, the platinum atoms form a thick film under the graphite monolayer, which is chemically strongly bonded to iridium and at the same time bonded to the graphite monolayer by van der Waals forces (Fig. 9b). This is the probable explanation of the *biintercalation effect* which we have discovered:[36] the successive adsorption of platinum atoms and then cesium atoms under the graphite monolayer is accompanied by the growth of a thick platinum film on which a cesium monolayer is formed (Fig. 10).

The condition $\varkappa=1$ means that a platinum atom that is physisorbed on the graphite monolayer succeeds in migrating during the desorption lifetime from the center of the graphite layer to its edge, which is possible if the migration of the platinum atoms over the graphite monolayer is very

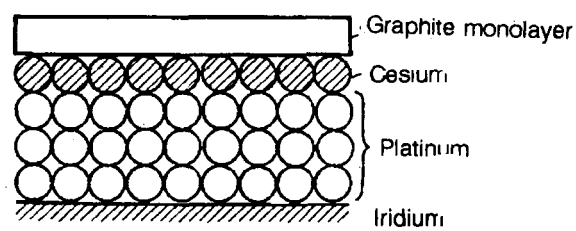

FIG. 10. Model structure of intercalated film in the case of biintercalation: successive adsorption of platinum atoms on a graphite monolayer on iridium at $T=1000$ K followed by adsorption of cesiumatoms at 300 K.

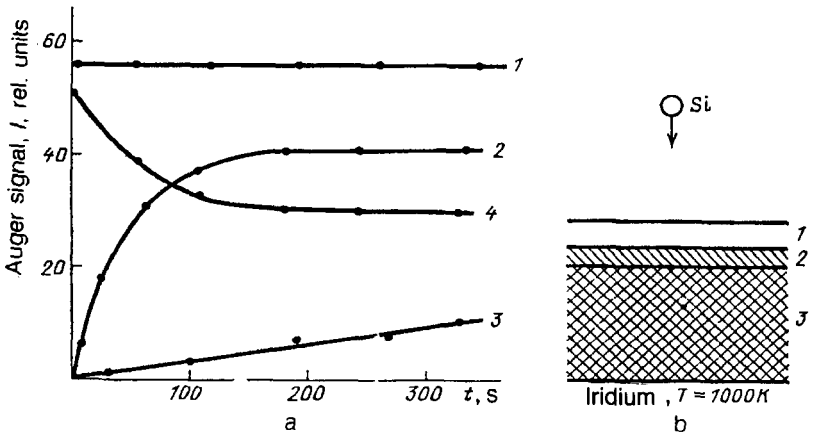

FIG. 11. a—Auger peak intensity for carbon (*1*), silicon (*2*), and iridium (*4*) as function of time of deposition of silicon on a monolayer of graphite on iridium at $T=1000$ K and the silicon Auger peak (*3*) for silicon deposited on Ir–C at 1500 K. b—Structure of intercalated films: *1*—two-dimensional graphite film, *2*—surface silicide, *3*—bulk silicide.

efficient. For this to happen, the graphite layer must be very smooth, the potential wells shallow, and the graphite islands relatively small. Since the platinum adatoms on the graphite monolayer on iridium are electrically neutral, they continue to be neutral when they decorate the edge of a graphite island, and platinum intercalation does not have the concentration threshold that is typical for the intercalation of Cs, K, Ba. This means that the initial fraction of adsorbed platinum atoms already penetrates under the graphite monolayer on iridium at 1000 K. In Ref. 36 we report important data on the efficiency of intercalation of Ir–C by platinum atoms at the lower temperatures of $300 < T < 1000$ K. When platinum is deposited on a graphite monolayer on iridium at 300 K, intercalation does not occur at room temperature and a monolayer of adsorbed platinum is formed with $N_{Pt} \sim 10^{15}$ cm^{-2}. This monolayer reduces the carbon Auger peak at $E=272$ eV by a factor of 1.5 and the iridium Auger peak $E=54$ eV by a factor of about 3. The temperature was then raised in steps of 100°, maintaining it for 30 s at each value of T. It was found that the iridium Auger peak remained unaltered as T was increased, but the carbon Auger peak grew by a factor of 1.5. This means, that, as the temperature T is raised, we find that, for $T < 1000 <$ K, for which the platinum has still not desorbed, the *entire* monolayer of adsorbed platinum already seems to be in the intercalated state.

2.6. Intercalation of Ir–C by silicon[36]

Silicon was deposited by sublimation from heated strips. Adsorption of silicon on Ir–C at 300 K is accompanied by the appearance of a thick silicon film on the surface, which reduces the height of the carbon and the iridium Auger peaks down to the background level. The growth of the silicon film undergoes a significant change as the temperature is raised. Figure 11a shows the variation in the height of the carbon, silicon, and iridium Auger peaks during adsorption of silicon on Ir–C at 1000 K. The growth of the silicon Auger peak suggests that silicon accumulates in the surface region, whereas the constancy of the carbon Auger peak indicates that silicon accumulates under the graphite monolayer. The silicon and iridium Auger peak cease to vary after 150 s of deposition, so that the composition of the $\geqslant$10–15 Å surface layer explored by AES also ceases to change. Special experiments[37] on the adsorption of silicon on pure iridium reveal that, for temperatures in the range $800 < T < 1400$ K and for concentrations up to $N_{Si} = 3 \times 10^{14}$ cm^{-2}, the entire silicon arriving on the surface accumulates in the form of a surface chemical compound, namely, a surface silicide. Thereafter, new portions of silicon arriving on the surface are found to diffuse into the interior of the iridium and form the bulk silicide. For given silicon beam intensity (and allowing for the reduction in the silicon Auger-peak intensity in the graphite monolayer), the silicon Auger-peak intensity as a function of the deposition time on iridium and iridium covered with the graphite monolayer is practically the same at 1000 K. This means that silicon intercalates Ir–C at 1000 K with an efficiency approaching $\varkappa \sim 1$. During adsorption of silicon on Ir–C at the higher temperatures $T \geqslant 1300$ K, a substantial fraction of silicon passes to the intercalated state and the remainder is desorbed.

2.7. Intercalation of Ir–C by carbon[11]

Following experiments[36] in which it was found that platinum and silicon atoms intercalate a graphite monolayer on iridium at 1000 K with efficiency $\varkappa = 1$, it is interesting to extend the number of atoms capable of intercalation to the carbon atoms themselves. This was done by depositing a screen of C-atoms (produced by our special source that did not produce C-clusters) on a graphite monolayer on iridium at temperatures in the wide range $300 < T < 1800$ K. The resulting film was analyzed AES which showed that a thick carbon film was produced at all these temperatures, but its character (graphite or a nongraphite) and its growth mechanism were very sensitive to temperature.

The adsorption of C-atoms on a graphite monolayer on iridium heated to $T < 700$ K is accompanied by the formation of a thick carbon film with nongraphite structure (Fig. 12). This is indicated by a number of characteristics. First, there is the shape of the C_{kvv} Auger peak (graphite is characterized by two peaks at 247 and 263 eV, respectively, whereas chemisorbed carbon has only one peak at 255 eV). Second, the adsorption of C-atoms on such a film does not produce the characteristic splitting of the C_{kvv} Auger peak (this will be discussed in Sec. 2.10) observed during the

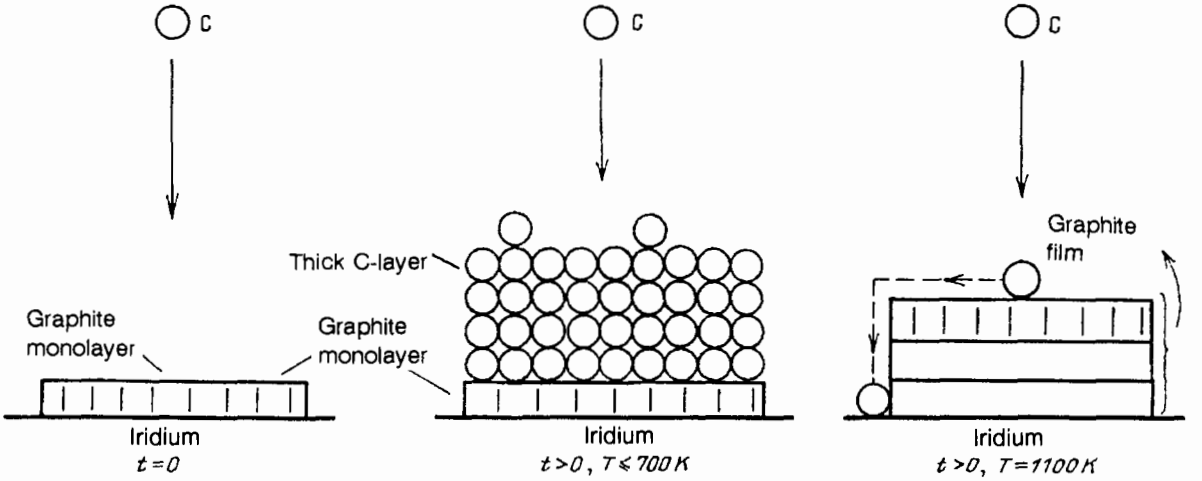

FIG. 12. Schematic structure of the C-film during adsorption of carbon atoms on a graphite monolayer on iridium at $T<700$ K and $T=1100$ K.

adsorption of cesium atoms on a graphite film. Third, the work function increases from 4.45 eV (typical for graphite) to 4.75 eV (typical for chemisorbed carbon). Fourth, the degree of dissociation of the CsCl molecules rises from 10^{-4} on the graphite monolayer to 0.1 on the thick carbon film. Consequently, the adsorption of the C-atoms on the graphite monolayer on iridium heated to 700 K is accompanied by the formation of a thick nongraphite carbon film that grows under the graphite monolayer without the intervention of the intercalation mechanism.

The carbon film is formed in a quite different way during the adsorption of C-atoms on a graphite monolayer on iridium at the higher temperature of 1100 K (Fig. 12). No accumulation of carbon was found in the adlayer and all the C-atoms reaching the surface either intercalate the graphite islands or are desorbed. Intercalation begins with the formation under the graphite monolayer of graphite islands in the adlayer on iridium and, after their coalescence, with the formation of a second graphite layer under the first. Once the second graphite layer is formed, the rate of growth of the third graphite layer falls by a factor of 3–5. This is so because the C-atoms that act as the building blocks must diffuse from the top of the film towards base, i.e., the surface of iridium, where they initiate graphite islands of the next layer, and this in turn leads to the loss of C-atoms by desorption and to a reduction in the rate of growth of the film. We note, by the way, that for $E<700$ K the rate of growth of the film remains constant for $\nu_C=\text{const}$. It follows that carbon does not accumulate in the adlayer during the adsorption of C-atoms on Ir–C at 1100 K: instead, it accumulates in the intercalated state under the graphite monolayer where the thick carbon film with a graphite structure is growing.

2.8. Intercalation of Ir–C by silver

Silver was deposited by sublimation from silver wires wound on a hot tungsten spiral. The adsorption of silver on a graphite monolayer on iridium did not give rise to intercalation at any temperature: a thick silver film was produced at $T<900$ K and the silver atoms were desorbed at $T>900$ K. It is possible that, because of their marked tendency to aggregate, the silver atoms form Ag_2, Ag_3 clusters at the edge of a graphite island in the starting position for intercalation and thus impede the penetration of silver under the islands.

However, if we first intercalate Ir–C with cesium atoms with $N\sim 2\times 10^{14}$ cm^{-2}, and then deposit a thick silver film at 300 K and raise the temperature to 1000 K, we find that silver in amounts equivalent to about a monolayer will efficiently flow under the graphite layer, and the remaining silver will desorb. Evidently, silver flows under the graphite islands when their edges are lifted, and displaces intercalated cesium.

2.9. Intercalation of Ir–C by copper, iridium, and molybdenum

Iridium and molybdenum are deposited by sublimation from wires, and copper was deposited from a hot tungsten spiral. As in the case of platinum atoms, the molybdenum, copper and iridium adatoms readily appear under the graphite monolayer, either when they are deposited on the substrate at 1000–1200 K or when thick films of the corresponding metals produced at 600 K were annealed at 1000–1200 K.

2.10. Electronic properties of a graphite monolayer on a metal with adsorbed and intercalated atoms

It is well-known that the densities of filled and unfilled electron states of two-dimensional graphite fall dramatically near the Fermi level. This is indicated by calculations[38,39] and has been confirmed by studies on the valence band of single-crystal graphite by photoelectron[40] and Auger electron[41,42] spectroscopy.

We shall use the Gurney scheme[43] to describe the interaction between particles and the surface of a metal. As an isolated atom approaches the surface of a metal, the discrete state of the valence electron in the atom expands to

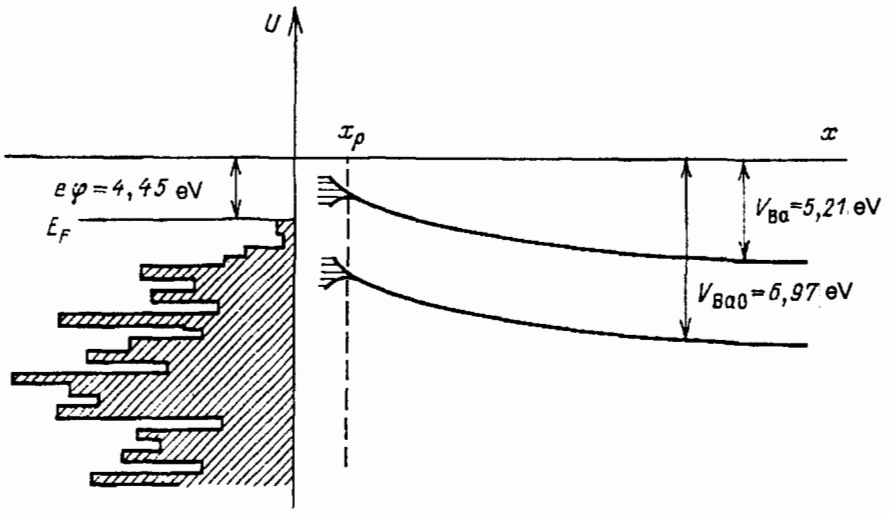

FIG. 13. Diagram illustrating the transformation of the energy level of a valence electron of a barium atom and the BaO molecule as the particle approaches the monolayer on a metal ($e\varphi$ is the work function and V is the ionization potential).

a quasilevel and shifts from its initial position (Fig. 13). In this scheme, different types of adatom differ only by the shape and position of the quasilevel. The charge of the adatoms is determined by the position of the center of the quasilevel relative to the Fermi level and by the width of the quasilevel. In both cases, a substantial portion of the quasilevel must lie above the Fermi level in order to ensure that there is an effective transfer of valence electrons from the cesium and barium adatoms to the graphite valence band. It is reasonable to expect that the C_{kvv} Auger transition in the two-dimensional graphite layer, in which two valence-band electrons participate, will be sensitive to the filling of the band. The electronic properties of Re–C and Ir–C containing cesium and barium were investigated in Refs. 14, 18, 20–23, and 27–28.

On the graphite monolayer deposited on a metal there are two types of atoms, namely, atoms adsorbed and intercalated under somewhat different conditions. We begin with the experiments reported in Ref. 28 in which high-resolution AES ($\Delta E/E \approx 0.1\%$) was used to examine the adsorption of barium atoms on a two-dimensional graphite film on iridium at 900 K. It was found that the barium was confined exclusively to the intercalated state up to concentrations of about 5×10^{14} cm^{-2} during saturation. It is clear from Fig. 14 that, prior to intercalation, the C_{kvv} Auger peak has the typical graphite shape with energies of 247 and 263 eV in the positive part of the spectrum and the absence of the carbide peak at 255 eV (spectrum *1*). It is clear that intercalation of barium does not affect the positive "graphite" part of the spectrum, whereas in the negative part the increase in the concentration of barium is accompanied by the appearance of a peak at 276.5 eV (spectra *2* and *5*) and then a second peak at 281 eV (spectra *3* and *4*). Hence it may be concluded that the intercalated barium is in the charged state and its valence electron is transferred to the graphite valence band and fills levels adjacent to the Fermi level. This is reflected in the change in the high-energy part of the C_{kvv} Auger peak, since in carbon the transition type is *kvv* and involves two electrons from the graphite valence band. An analogous picture is observed during the intercalation of HOPG by alkali-metal atoms.[41,42] After the Ir–C strip was heated to 1600 K, some of the intercalated barium was desorbed and the remaining concentration of barium was 2×10^{14} cm^{-2}, which corresponds to the Auger peak at 276.5 eV (spectrum 5).

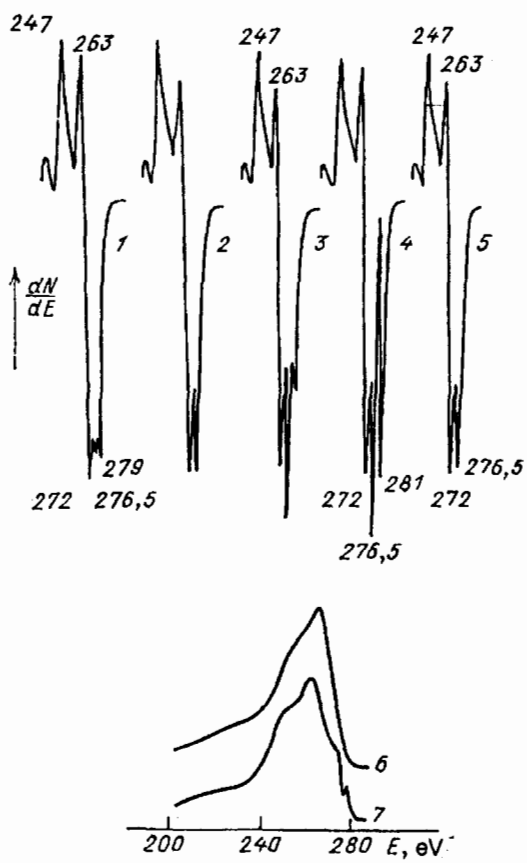

FIG. 14. Auger spectra of carbon in differential form (*1–5*) during the adsorption of barium on a carbon monolayer on iridium at 900 K; concentration of barium in the γ-phase N_γ (cm^{-2}): *1*—0.2, *2*—$1.5\cdot10^{14}$, *3*—$2.5\cdot10^{14}$, *4*—$5.0\cdot10^{14}$ (adsorption to saturation); *5*—Auger spectrum of carbon after heating of state 4 to 1600 K ($N_\gamma \sim 2\times10^{14}$ cm^{-2}), b—Auger spectrum of carbon in integral form for a graphite monolayer on iridium, *7*—Auger spectrum of carbon in integral form for the state *4*.

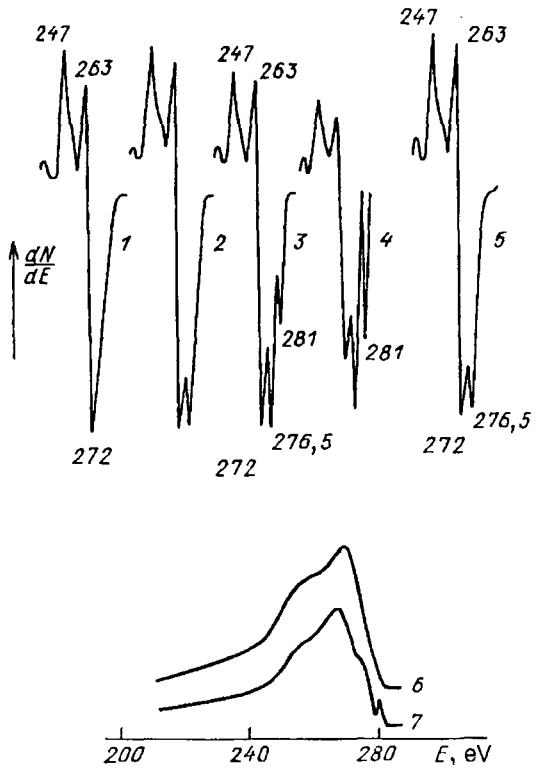

FIG. 15. Auger spectra of carbon in differential form (*1–5*) during adsorption of cesium on a graphite monolayer on rhenium at 300 K; cesium concentration $N_\alpha+N_\gamma$ (cm^{-2}): *1*—0, *2*—$1\cdot10^{14}$, *3*—$2\cdot10^{14}$, *4*—$7.5\cdot10^{14}$, (adsorption to saturation) *5*—Auger spectrum of carbon after heating in state *4* to 850 K ($N_\gamma\sim10^{14}$ cm^{-2}, *6*—Auger spectrum of carbon in integral form for graphite monolayer on rhenium, *7*—Auger spectrum of carbon in integral form from state *4*.

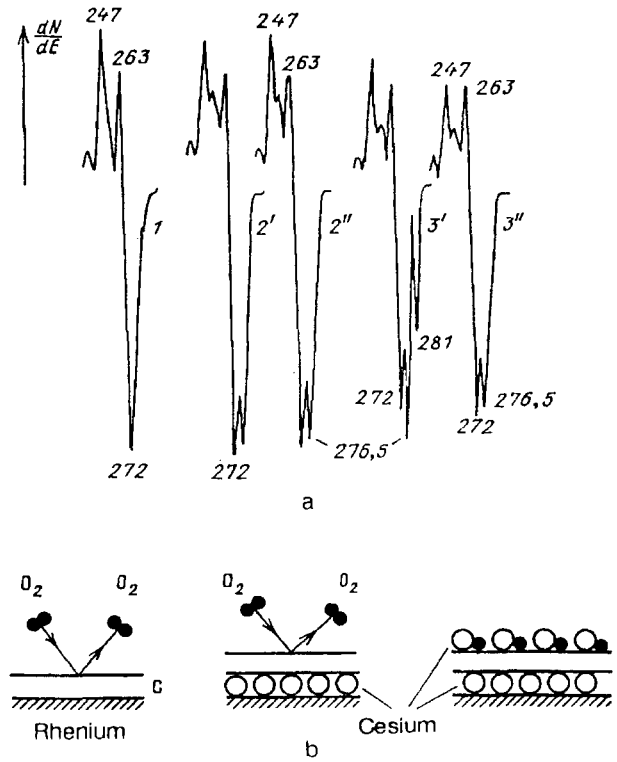

FIG. 16. Auger spectra of carbon during adsorption of cesium on graphite monolayer on rhenium at 300 K. Concentration of cesium in the α- and γ-phase $N_\alpha+N_\gamma$ (cm^{-2}): *1*—0, *2*—$1.5\cdot10^{14}$, *3*—$7\cdot10^{14}$. Spectra *2'* and *3'* recorded prior to exposure to oxygen; spectra *2''* and *3''* recorded after the exposure (dose$=10^{-6}$ Torr$\times$60 s$=60L$).

Figure 15 shows[28] the C_{kvv} Auger spectra due to the adsorption of cesium on Re–C. There is a simultaneous filling of the adsorbed (concentration N_α) and intercalated (concentration N_γ) states, and at the end of adsorption but prior to saturation we have $N_\alpha\sim N_\gamma\sim4\times10^{14}$ cm^{-2}. It is clear that the valence electrons in cesium occupy the same levels in the graphite valence band as in the case of barium adsorption, and the negative part of the spectrum contains both the 272-eV peak and the peaks at 276.5 and 281 eV.

Interesting information on the intercalation of cesium and barium was obtained in Ref. 28 when oxygen was admitted into the system. Re–C containing only intercalated cesium or adsorbed and intercalated cesium at 300 K was kept in oxygen (10^{-6} Torr$\times$60 s$=60L$) and the C_{kvv} Auger spectra were recorded (Fig. 16). It was found that the concentration of surface oxygen on the graphite monolayer at 300 K was low and was not recorded by AES (it had been shown[44] that oxygen is physisorbed only on the basal plane of the graphite crystal). During the exposure to oxygen, the shape of the C_{kvv} Auger peak of intercalated cesium remained constant, i.e., oxygen did not diffuse under the graphite islands on rhenium. At the same time, the shape of the C_{kvv} Auger peak due to adsorbed cesium underwent a change: the 281-eV peak vanished, showing that oxidation was accompanied by the return of some cesium valence electrons from the graphite valence band to the oxide molecule. Figure 13 illustrates this in the case of barium: oxidation of a barium adatom on the graphite monolayer produces the admolecule BaO with its own set of electron levels. It may be expected that, since the ionization potential of the BaO molecule is high (6.97 eV as compared with 5.21 eV in the case of the barium adatom), the quasilevel occupied by the valence electron in the admolecule BaO lies below the graphite Fermi level, so that it is filled during oxidation by electrons from the graphite valence band.

In Ref. 28 we examined the interesting possibility of intercalation by cesium of the surface of iridium bearing a graphite monolayer and a monolayer of chemisorbed carbon with concentration $N_C\sim3.9\times10^{15}$ cm^{-2}, produced by the adsorption of C-atoms on iridium at 300 K. We found that, in contrast to the graphite monolayer, cesium does not intercalate the monolayer of chemisorbed carbon: the characteristic splitting of the C_{kvv} Auger peak does not occur and the high-temperature γ-phase ($T>2000$ K) is absent from the thermal desorption spectrum.

We have investigated intercalation of not only the two-dimensional graphite film, but also of the thicker graphite films on metals. For example, Fig. 17, taken from Ref. 21, shows the C_{kvv} Auger peaks during the intercalation by cesium of a thick $n=4$ graphite film on Re (spectrum *3*). These are similar to the corresponding peaks obtained for

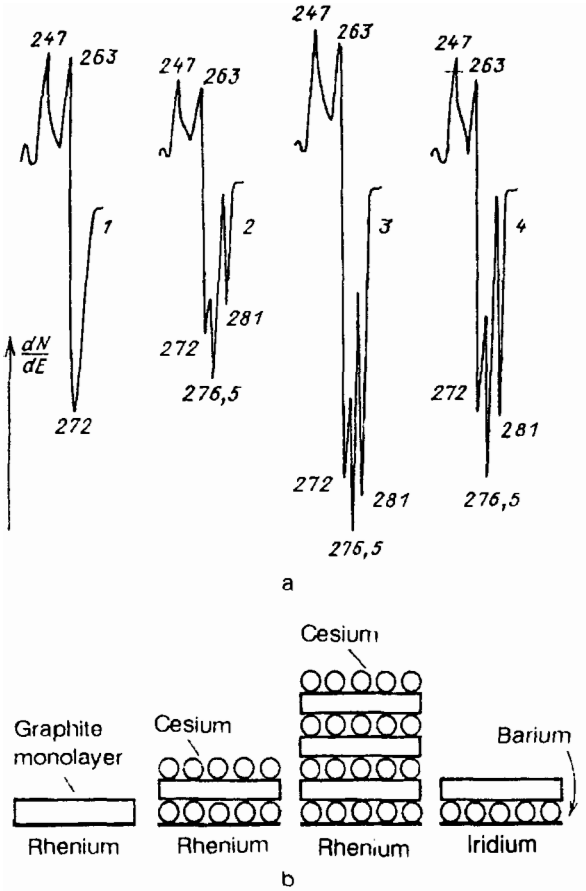

FIG. 17. a—Auger spectra of carbon from a graphite monolayer on rhenium before (*1*) and after (*2*) adsorption of cesium atoms at 300 K to saturation ($N_\alpha+N_\gamma\approx 8\times 10^{14}\ \mathrm{cm}^{-2}$); *3*—Auger spectrum of carbon from a thick ($n=4$) graphite film on rhenium, intercalated by cesium at 300 K to saturation; *4*—Auger spectrum of carbon from a graphite monolayer on iridium, intercalated by barium atoms at $T\approx 900$ K ($N_\gamma\approx 5\times 10^{14}\ \mathrm{cm}^{-2}$). b—Schematic disposition of cesium and barium atoms.

the intercalation by cesium of a graphite monolayer on rhenium (spectrum *2*) or barium on a graphite monolayer on iridium (spectrum *4*). We found that a thick film of this kind is completely intercalated by cesium at 300 K. When the film is held in oxygen at 300 K, the carbon Auger peak becomes much weaker, but the cesium Auger peak is considerably enhanced and there is also a strong oxygen Auger peak. Oxygen is thus seen to produce the expected effect, namely, the stimulated release of the intercalate on the graphite film surface and its oxidation. We assume that when the outer face of the graphite film is oxidized, the cesium adatoms are neutralized and cease to impede the migration of Cs^+ ions from the interior of the graphite film where the cesium atoms are charged and are repulsed by Coulomb forces. This is accompanied by the growth of an oxide of the alkaline metal to a considerable thickness on the outer force of the graphite film.

3. PHYSICS OF INTERCALATION

To understand the reasons for the high efficiency with which different atoms intercalate a two-dimensional graphite film on a metal, we have to establish the type of bonding that exists between a graphite island and the surface of the metal. This fundamental problem was examined in an original way in a chapter of the monograph entitled *Carbon on the Surface of a Transition Metal*, by A. Ya. Tontegode.[1] Obviously, the electronic properties of contacting particles have to be taken into account in any explanation of the bonding between them. We know that the graphite single crystal has a layered structure: it consists of two-dimensional graphite layers. The C-atoms in a layer are coupled by strong chemical bonds, which means that the relatively high energy of about 9 eV has to be supplied to remove an atom from the interior of the graphite layer. Moreover, the C-atoms are closely spaced and have a very small atomic radius $R_c\approx 1.4$ Å/2=0.7 Å. Weak van der Waals forces of polarization origin (physisorbtion without electron exchange) operate between the graphite layers, and the separation between the layers is relatively large. The corresponding effective van der Waals radius is large, $R_{B\text{-}B}=3.35/1.67$ Å which is greater by about 1 Å than the atomic radius of carbon.

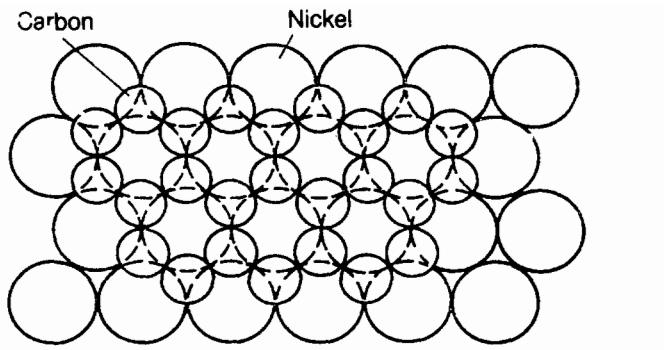

FIG. 18. Structure of the Ni (111) face with an adsorbed graphite monolayer.

It is shown in Ref. 1 that the character of the bonding between the graphite islands and the surface of a metal can be established by analyzing the measured separation I_{meas} between the centers of C-atoms in the graphite layer and the centers of atoms in the surface layer of the metal. Consider the system Ni (111) plus a graphite monolayer, investigated by SEELFF and LEED in Ref. 45. We note that the (111) surface of Ni is unique among the transition metals because its crystal geometry provides an excellent match to the structure of the graphite layer (Fig. 18). It is only on this surface that we can have the precise graphite monolayer in which two carbon atoms correspond to one surface Ni atom when all the identical adsorption centers, i.e., wells between Ni atoms on the surface, are occupied by C-atoms. LEED experiments have shown that an ordered 1×1 picture is indeed formed on Ni (111) and that the C-atoms are located in the wells on this surface. SEELFS was used to obtain the important result $L_{meas}=2.80\pm 0.8$ Å for the separation between the centers of C-atoms in the graphite layer and the centers of Ni atoms on the surface, but the authors of Ref. 45 did not examine the reasons for this result. In chemisorption, in which electron exchange

occurs between the contacting objects, the distance L_{meas} between the centers of C-atoms and the centers of Ni atoms on the surface can be estimated graphically by placing the C-atoms with the Ni atoms on the surface with atomic radii $R_{Ni}=1.24$ Å. It is found that $L_{chem}<1.6$ Å. In physisorption, in which there is no electron exchange between the graphite monolayer and the nickel surface, the graphite monolayer on the surface of the metal is in a state similar to that in the graphite crystal, i.e., it exists in the form of a plate of thickness $2R_{B-B}=3.35$ Å whose center is shifted from the plane passing through the centers of the surface nickel atoms by the amount $L_{phys}=R_{B-B}+R_{Ni}=1.67+1.24=2.91$ Å. Since A_{meas} is in good agreement with L_{phys}, this must mean that the graphite monolayer is in fact physisorbed on the Ni (111) surface.

Dynamic DME was used in Ref. 46 to examine Pt (111) with surface carbon produced by exposing platinum at 1100 K to propylene (C_3H_5). It was found that the graphite monolayer was in contact with C-atoms chemisorbed on the Pt (111) surface and that $L_{meas}=2.45$ Å between the centers of the chemisorbed C-atoms and the centers of C-atoms in the graphite monolayer. For physisorption of the graphite monolayer on surface carbon atoms, $L_{phys}+R_{B-B}+R_C=1.67+0.7=2.37$ Å. Since L_{phys} is in good agreement with L_{meas}, we consider that the graphite monolayer is physisorbed on the surface carbon atoms on Pt (111) and not as suggested in Ref. 46 where this bonding is interpreted as a hybrid of physisorption and chemisorption.

We consider that the graphite single crystal is a body with valence saturated surfaces. The corresponding idealogy is developed in Ref. 47. Surface atoms on such bodies have no free orbitals with the unpaired electron that are necessary for covalent bonding to the adparticles. Evidence for valence saturation is provided by the presence in the solid phase of regions coupled by van der Waals forces, e.g., as in the layered structures such as graphite, MoS_2, $TaSe_2$, CdI_2, Bi_2Te_3,... . Actually, if there were free valence bonds perpendicular to a graphite layer in single-crystal graphite, the layer separation would be $2R_C=1.4$ Å which is typical for covalent bonds. Because of valence saturation in the two-dimensional graphite layer, the true layer separation is $2R_{B-B}=3.35$ Å, i.e., it is greater by about 2 Å. It is therefore reasonable to expect that the valence-saturated graphite monolayer is physisorbed on the surface of any metal, independently of its crystal geometry and nature. The detection of graphite islands on the surface of most transition metals[48–52] confirms their physisorption on metals. In fact, in the course of chemisorption, the minute carbon atoms bound strongly to the metal surface cannot form a graphite monolayer because the crystal geometry of the metal surface [other than the Ni (111) surface] cannot be matched to the structure of the graphite layer.

The mechanism of intercalation by atoms of the two-dimensional graphite film on metals is of considerable scientific and practical interest because, on the one hand, it should enable us to gain a deeper understanding of the physicochemical nature of the phenomenon and, on the other hand, by revealing the properties of the particles taking part in intercalation, it should help us to extent the range of intercalated systems. It may well be that the mechanism of intercalation of a two-dimensional graphite film on metals will be amenable to extension to the intercalation of massive graphite (HOPG) and other layered systems (MoS_2...).

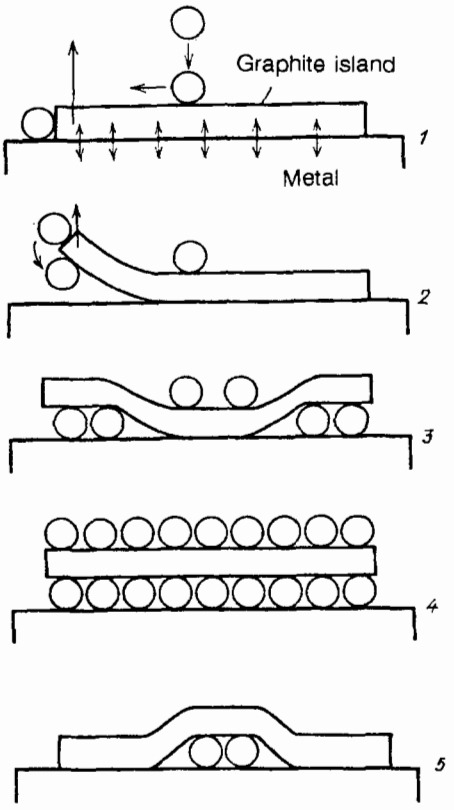

FIG. 19. Schematic diagram illustrating the successive stage of intercalation.

An intercalation mechanism is developed in Ref. 13 for the atoms of a two-dimensional graphite film on a metal. It is based on account being taken of the random thermal motion of C-atoms in the graphite layer. A new model of a graphite island in the adlayer of a metal is also proposed in Ref. 13: an island is represented by a solid disk of thickness $h=3.35$ Å which can be reduced by applying external pressure in a way similar to the compression of a graphite crystal by external pressure.[53] The graphite island is held against the surface by weak van der Waals forces. In the course of adsorption of, say, a cesium atom (atomic radius 2.68 Å, ionic radius 1.65 Å) on a graphite island on a metal, the atom migrates over the surface of the island and places itself at its edge, in the starting position for intercalation. Figure 19 illustrates the situation prior to intercalation: the large cesium adatom must penetrate under the edge of the thick solid graphite plate held against the metal. It is assumed that, during its random thermal motion, each C-atom in the graphite layer can accumulate sufficient kinetic energy during its motion over the surface to break its bonding to the surface and to several neighboring C-atoms. The result of this is a "bubble" in the

graphite island, with the intercalated atoms migrating over its inner surface. Bubbles continually appear and disappear at points in the island. A bubble must be formed at the edge of the island for the intercalation of a particle start. If the bonding between particle and the edge of an island is stronger than the bonding to the metal, the particle finds itself at the edge of the island when the bubble is formed. In the opposite case, the particle is on the surface of the metal and migrates under the island. During adsorption, the intercalate populates the island edge regions whilst the central portion of the islands descends on to the metal. At the end of the adsorption process, the particles fill the intercalated and adsorbed state over the entire surface of the island. When this system is heated, all the cesium atoms are desorbed at about 800 K, and so are some of the intercalated atoms lying near the island edge. The van der Waals forces then bring the island edges down on to the surface and prevent the migration of the intercalated atoms from the center of the island. These atoms succeed in escaping only at the very high temperatures $T > 2000$ K when the islands dissolve in the adlayer, staring with the edges.

The intercalation mechanism was described in Ref. 13 for the first time in terms of the Frenkel' formula $\tau = \tau_0 \exp(E/kT)$, which gives the average particle lifetime, e.g., the desorption lifetime, where E is the desorption activation energy and T is the temperature. In traditional applications of the Frenkel' formula to desorption, a particle in random thermal motion acquires kinetic energy E which, at the end of the time τ, is equal to the desorption activation energy, and is desorbed. The Frenkel formula was used in Ref. 13 for another purpose, namely, to calculate the kinetic energy E acquired during the thermal motion by a bonded particle in a given time of observation τ at given temperature T. It is precisely this energy that is significant in the intercalation model because it is drawn upon when a bubble is created. For example, for $T = 300$ K and $\tau = 1$ s, the energy acquired by each C-atom in a graphite bonded to the substrate is $E = 0.78$ eV (for $\tau_0 = 10^{13}$ s) whereas for $\tau = 1000$ s, the energy is $E = 0.95$ eV. The energy stored in bonds increases rapidly with increasing temperature and rises to $E = 3.9$ eV when $T = 1500$ K and the observing time is $\tau = 1$ s. Suppose, for example, that the bonding energy between the substrate and the C-atom in a physisorbed graphite island on a metal is 0.2 eV. A graphite bubble will then contain about 4 atoms at 300 K, but a large graphite bubble containing about 20 atoms will be produced at 1500 K.

These estimates show that the essential condition for efficient intercalation is weak bonding between the graphite island and the metal surface. Actually, when a C-atom is chemisorbed to a substrate with a high bonding energy (for example, 6.0 eV), a bubble will not be formed even at the 1500 K necessary for intercalation because the accumulated energy is not sufficient. Experiment has confirmed these ideas. To demonstrate this, a monolayer of chemisorbed carbon was deposited on iridium with C-atom desorption energy of about 6.0 eV and concentration of about 3.9×10^{15} cm^{-2}, i.e., the same as in graphite. If we adsorb potassium atoms on the monolayer of chemisorbed carbon at 300 K, intercalation will not take place. If iridium with surface carbon is heated to 1600 K, it will be graphitized and intercalation by potassium will take place. At the instant of intercalation, the bubble mechanism will produce groups of atoms under the two-dimensional graphite film, rather than a uniform distribution of these atoms.

Let us now examine why the intercalated particles remain for a long time under the island at the high temperatures $T \approx 2000$ K. Suppose that, at 300 K, the concentration of graphite islands in the adlayer on the metal is $n = 10^8$ cm^{-2} and the concentration of the intercalated potassium is $N = 4 \times 10^{14}$ cm^{-2}. We then have 4×10^6 potassium atoms under one graphite island and the island occupies an area with linear dimensions of 2000 potassium atoms by 2000 potassium atoms. As the temperature T is raised to 1000 K, 75% of the intercalated potassium is desorbed whilst 25% remains under the center of the island occupying an area of 1000 potassium atoms times 1000 potassium atoms. A large empty space thus appears between the edge of the graphite island and the edge of the intercalated potassium island. This space could be filled by 500 potassium atoms on each side. It follows that if the linear size of the bubble is appreciably smaller than this distance, the potassium atoms will not leave through the edges of the graphite islands held by van der Waals forces against the metal surface.

We note that the new application of the Frenkel' formula[13] to calculations of the kinetic energy stored in a bond during the thermal vibrations of a particle can also be used to solve this type of problem.

4. CONCLUSION

The technology of fabrication and characterization of two-dimensional graphite films on metal surfaces was exploited in recent years in the discovery of the phenomenon of intercalation of these films by atoms. Detailed and fundamentally new data on the intercalation process have been obtained. It has been shown that atoms with low ionization potential (Cs, K, Ba,...) form a two-dimensional film in the intercalated state, whereas atoms with high ionization potential (Pt, Si, C,...) form a thick multilayer film. Analysis of experimental data has led to the development of models and has revealed some important characteristics of these objects. It is expected that an increase in the number of available intercalated atoms and a transition to the intercalation molecules (C_{60} etc.) as well as the use of nonmetallic substrates (silicon etc.) should lead to further advances in this field.

The experimental material presented above shows convincingly that, even now, the intercalation by atoms of a two-dimensional graphite film on a metal is a powerful method of synthesizing new film materials with unusual properties. For example, Ref. 54 reports the discovery of superefficient diffusion of potassium atoms intercalated on Ir–C into iridium. This is based on the surprisingly high thermal stability of the intercalated potassium atoms ($T_{des} > 2000$ K). It is found that, at high temperatures $T \sim 1700$ K, up to 25% of potassium atoms incident on a

graphite monolayer on iridium should diffuse into the latter. This is greater by a factor of about 10^8 than the efficiency of diffusion of potassium into iridium with a carbon-free surface. The superefficient diffusion of intercalated atoms into a metal can be exploited in the active doping of the surface layers of metals with atoms, thus producing new materials with unique properties.

The above experimental data and physical ideas on the intercalation by different atoms (Cs, K, Ba, Sr, Pt, Si, C, Ag, Cu, Ir, and Mo) of a two-dimensional graphite film on a metal will be useful in studies of new carbon materials based on the recently discovered family of fullerene molecules that consist exclusively of carbon molecules.[55] For example, they will assist us in gaining a better understanding of the transport of atoms over the surface of carbon nanotubules whose straight portion consist of graphite hexagons whilst the curvilinear portion consist of a mixture of hexagons and pentagons, and probably has the fullerene structure.

[1] A. Ya. Tontegode, Prog. Surf. Sci. **38**, 201 (1991).
[2] E. Ya. Zandberg, A. Ya. Tontegode, and F. K. Yusifov, Zh. Tekh. Fiz. **42**, 171 (1972) [Sov. Phys. Tech. Phys. **17**, 134 (1972)].
[3] E. V. Rytov and A. Ya. Tontegode, Pis'ma Zh. Tekh. Fiz. **7**, 1122 (1981) [Sov. Tech. Phys. Lett. **7**, 480 (1981)].
[4] E. V. Rytov and A. Ya. Tontegode, Zh. Tekh. Fiz. **52**, 921 (1982) [Sov. Phys. Tech. Phys. **27**, 589 (1982)].
[5] M. S. Dresselhaus and G. Dresselhaus, Adv. Phys. **30**, 139 (1981).
[6] M. S. Dresselhaus (ed.), *Intercalation in Layered Materials*, NATO ASI-Physics B, 148 (1986).
[7] D. Davidov and H. Selig (eds.), *Graphite Intercalation Compounds*, Proc. Fourth Internat. Symp. on Graphite Intercalation Compounds, Jerusalem, 1987; Synth. Metals **23**, 534 (1988).
[8] K. Luders and R. Schöllhorn (eds.), Proc. Fifth Internat. Symp. on Graphite Intercalation Compounds, Berlin, 1989; Synth. Metals **34**, 1–762 (1989–1990).
[9] D. Tchoubar and J. Conard (eds.), Proc. Sixth Internat. Symp. on Graphite Intercalation Compounds, Orleans, 1991; Mater. Sci. Forum **91–93**, 1–854 (1992).
[10] H. Zabel and S. A. Solin (eds.), *Graphite Intercalation Compounds*, Springer Ser. Mater. Sci. **14** (1990); **18** (1992).
[11] A. Ya. Tontegote, in *Chemical Physics of Intercalation II*, P. Bernier, J. E. Fischer, S. Roth, and S. A. Solin (eds.), Nato ASI Ser. B: Physics, **305** (1993).
[12] A. Ya. Tontegote, *Abstracts of Seventh Symp. on Intercalation Compounds*, Louvain-la-Neuve, 10–14 May, 1993.
[13] A. Ya. Tontegote, Pis'ma Zh. Tekh. Fiz. **15**, 57 (1989).
[14] N. A. Kholin, E. V. Rut'kov, and A. Ya. Tontegote, Surf. Sci. **139**, 155 (1984).
[15] N. I. Ionov and E. Ya. Zandberg, *Surface Ionization* [in Russian], Nauka, Moscow, 1969.
[16] E. Ya. Zandberg, E. N. Nazarov, U. Kh. Rasulev, E. V. Rut'kov, and A. Ya. Tontegote, Zh. Tekh. Fiz. **52**, 746 (1982) [Sov. Phys. Tech. Phys. **27**, 472 (1982)].
[17] N. R. Gall', S. N. Mikhaĭlov, E. V. Rut'kov, and A. Ya. Tontegote, Fiz. Tverd. Tela **27**, 2351 (1985) [Sov. Phys. Solid State **27**, 1410 (1985)].
[18] N. R. Gall', S. N. Mikhaĭlov, E. V. Rut'kov, and A. Ya. Tontegote, Zh. Tekh. Fiz. **56**, 732 (1986) [Sov. Phys. Tech. Phys. **31**, 441 (1986)].
[19] N. R. Gall', S. N. Mikhaĭlov, E. V. Rut'kov, and A. Ya. Tontegote, Surf. Sci. **191**, 185 (1987).
[20] N. R. Gall', S. N. Mikhaĭlov, E. V. Rut'kov, and A. Ya. Tontegote, Fiz. Tverd. Tela **28**, 2521 (1986) [Sov. Phys. Solid State **28**, 1411 (1986)].
[21] N. R. Gall', S. N. Mikhaĭlov, E. V. Rut'kov, and A. Ya. Tontegote, Sunth. Metals **34**, 497 (1989).
[22] V. N. Ageev, E. V. Rut'kov, A. Ya. Tontegote, and N. A. Kholin, Fiz. Tverd. Tela **24**, 780 (1982) [**24**, 440 (1982)].
[23] N. R. Gall', S. N. Mikhaĭlov, E. V. Rut'kov, and A. Ya. Tontegote, Poverkhnost' No. 4, 22 (1987).
[24] E. Ya. Zandberg, M. V. Knat'ko, and V. I. Paleev, Pis'ma, Zh. Tekh. Fiz. **12**, 388 (1986) [Sov. Tech. Phys. Lett. **12**, 158 (1986)].
[25] N. R. Gall', S. N. Mikhaĭlov, E. V. Rut'kov, and A. Ya. Tontegote, Zh. Tekh. Fiz. **59**, 154 (1989) [*sic.*].
[26] A. Ya. Tontegote, R. M. Abdulayev, and F. K. Yusifov, Zh. Tekh. Fiz. **45**, 1904 (1975) [Sov. Phys. Tech. Phys. **20**, 1201 (1975)].
[27] N. R. Gall', S. N. Mikhaĭlov, E. V. Rut'kov, and A. Ya. Tontegote, Poverkhnost' No. 12, 14 (1986).
[28] N. R. Gall', S. N. Mikhaĭlov, E. V. Rut'kov, and A. Ya. Tontegote, Surf. Sci. **226**, 381 (1990).
[29] E. V. Rut'kov and A. Ya. Tontegote, Fiz. Tverd. Tela **32**, 2960 (1990) [Sov. Phys. Solid State **32**, 1718 (1990)].
[30] E. V. Rut'kov and A. Ya. Tontegote, in Proc. Sixth Internat. Symp. on Graphite Intercalation Compounds, Orleans, 1991, D. Tchoubar and J. Conard (eds.), Mater. Sci. Forum **91–93**, part 2, 709 (1992).
[31] E. Ya. Zandberg, E. V. Rut'kov, and A. Ya. Tontegote, Pis'ma Zh. Tekh. Fiz. **1**, 741 (1975) [Sov. Tech. Phys. Lett. **1**, 324 (1975)].
[32] E. Ya. Zandberg, N. D. Potekhina, E. V. Rut'kov, and A. Ya. Tontegote, Pis'ma Zh. Tekh. Fiz. **1**, 805 (1975) [Sov. Tech. Phys. Lett. **1**, 805 (1975)].
[33] E. Ya. Zandberg, E. V. Rut'kov, and A. Ya. Tontegote, Zh. Tekh. Fiz. **46**, 2610 (1976) [Sov. Phys. Tech. Lett. **21**, 1541 (1976)].
[34] E. Ya. Zandberg, E. V. Rut'kov, N. D. Potekhina, and A. Ya. Tontegote, Fiz. Tverd. Tela **19**, 1665 (1977) [Sov. Phys. Solid State **19**, 972 (1977)].
[35] E. Ya. Zandberg, E. V. Rut'kov, and A. Ya. Tontegote, *Abstracts of Seventeenth All-Union Conf. Emission Electronics* [in Russian], LIYaF AN SSSR, L., 1978, p. 95.
[36] N. R. Gall', E. V. Rut'kov, and A. Ya. Tontegote, Pis'ma Zh. Tekh. Fiz. **14**, 527 (1988) [Sov. Tech. Phys. Lett. **14**, 235 (1988)].
[37] N. R. Gall', E. V. Rut'kov, and A. Ya. Tontegote, Poverkhnost' No. 10, 47 (1989).
[38] G. S. Painter and D. E. Ellis, Phys. Rev. B **1**, 4747 (1970).
[39] R. F. Willis, B. E. Fitton, and G. S. Paintor, Phys. Rev. B **9**, 1926 (1974).
[40] D. Marchand, C. Fretigny, M. Lagües, F. Batallan, Ch. Simon, I. Roseman, and R. Pinxhax, Phys. Rev. B **30**, 4788 (1984).
[41] P. Pfluger, P. Oelhafen, N. H. Kunzi, R. Ieker, E. Hauser, K. P. Ackermann, M. Müller, and H. I. Güntherodt, Physica B+C **99**, 395 (1980).
[42] P. Oelhafen, P. Pfluger, and H. I. Güntherodt, Sol. State Commun. **32**, 885 (1979).
[43] R. Gurney, Phys. Rev. **47**, 479 (1935).
[44] J. J. Lander and J. Morrison, Appl. Phys. Lett. **35**, 3593 (1964).
[45] R. Rosei, M. De Crescenzi, F. Sette, C. Quaresima, A. Savoia, and P. Perfetti, Phys. Rev. B **28**, 1161 (1983).
[46] Hu Zi-Pu, P. F. Ogletree, M. A. van Hove, and G. A. Somorjai, Surf. Sci. **180**, 433 (1987).
[47] A. Ya. Tontegote, *Surface Ionization of Atoms and Molecules and Its New Applications* [in Russian], Abstracts of the Ioffe Physicotechnical Institute, Leningrad, 1974.
[48] T. W. Haas and J. T. Grant, Appl. Phys. Lett. **16**, 172 (1970).
[49] J. P. Coad and J. C. Riviere, Surf. Sci. **25**, 609 (1971).
[50] J. T. Grant and T. W. Haas, Surf. Sci. **24**, 332 (1971).
[51] J. C. Shelton, H. R. Patil, and J. M. Blakely, Surf. Sci. **43**, 493 (1974).
[52] B. E. Nieuwenhuys, D. I. Hagen, G. Rovida, and G. A. Somorjai, Surf. Sci. **59**, 155 (1976).
[53] M. Hanfland, N. Beister, and K. Syassen, Phys. Rev. B **88**, 303.
[54] A. Ya. Tontegote, Pis'ma Zh. Tekh. Fiz. **15**, 57 (1989).
[55] A. V. Eletskiĭ and B. M. Smirnov, Usp. Fiz. Nauk **163**, 633 (1993).

Translated by S. Chomet